LA-UR-21-28279
Approved for public release; distribution is unlimited.

Title: CFD Analysis of RLUOB Zone 1 HEPA Filter Plenum and Testing Manifolds

Author(s): Bari, Nadim Al

Intended for: Personal Archive
Report

Issued: 2021-08-18

Los Alamos NATIONAL LABORATORY

Memorandum

Engineering Technology and Design

To: John C. Sur, ES-EPD, MS M981
From: Nadim A. Bari, E1, MS J576
Phone: 505-412-5939
Symbol: E-1:21-016
Date: June 16, 2021

Subject: CFD Analysis of RLUOB Zone 1 HEPA Filter Plenum and Testing Manifolds

The purpose of this computational fluid dynamics (CFD) analysis is to ensure that Camfil Farr's upstream and downstream injection and sampling manifolds can meet or exceed the requirements outlined in the ASME AG-1 1997 a(2000) Code on Nuclear Air and Gas Treatment for the testing of HEPA and adsorbent filters.

This paper will present a numerical simulation of airflow in the Radiological Laboratory Utility Office Building (RLUOB) zone 1 HEPA filter plenum and testing manifolds using the commercial CFD software ANSYS FLUENT® 2020R1. The CFD analysis focuses on the investigation of the air flow distribution and air-aerosol mixing uniformity. The evaluation was done for all steps of the modeling process: grid generation, physics setup, simulation, and post-processing. The mass flow rate in each section of the zone 1 injection and sampling manifolds is also reported.

ASME AG-1 Requirements and Acceptance Criteria

A brief summary of the requirements for the housing and test section qualifications in accordance with AG-1 are defined below:

Air Flow Distribution

- Test requirement: while the system is operating at design flow rate, air flow distribution shall be measured downstream of the HEPA filter.
- Acceptance criteria: the variation in velocity measurements across the HEPA filter banks shall be limited to ±20% of the average velocity in each bank.

Air-Aerosol Mixing Uniformity

- Test requirement: while the system is operating at design flow rate, the air-aerosol mixing shall be measured upstream of the HEPA filter bank.
- Acceptance criteria: the variation in concentration of the air-aerosol mixture immediately upstream of the HEPA filter bank shall be limited to ±20% of the average concentration across all filters being tested.

Geometry and Computational Domain

SolidWorks® 2019 and ANSYS SpaceClaim® were used to model all geometries. The modeling process involved creating the geometries in SolidWorks® and importing them into ANSYS

SpaceClaim® to “repair and defeature” by extracting the fluid volume and removing short edges and sharp angles. The geometries used in this analysis are shown in Figures 1.1 – 1.3.

HEPA Filter Plenum

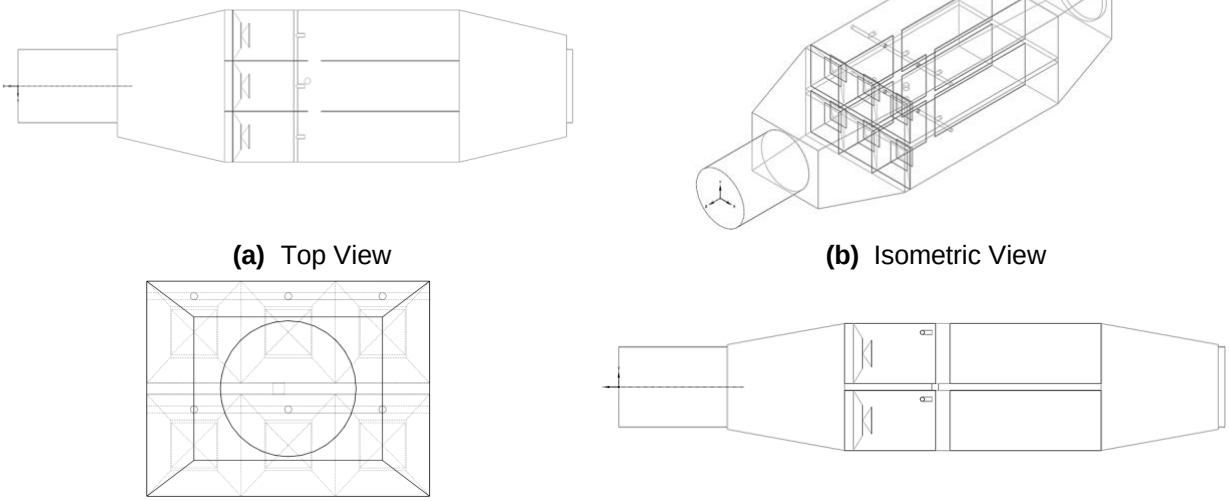

(a) Top View

(b) Isometric View

(c) Front View

(d) Side View

Figure 1.1: The top (a), isometric (b), front (c), and side (d) view of the HEPA filter plenum is shown.

Zone 1 Injection Manifold

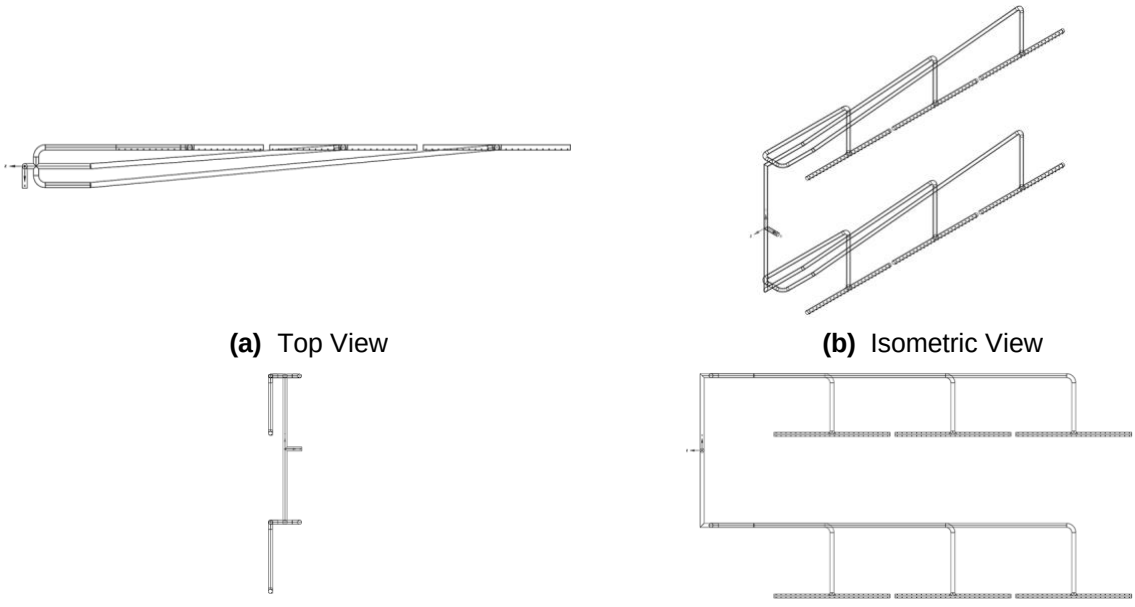

(a) Top View

(b) Isometric View

(c) Side View

(d) Downstream View

Figure 1.2: The top (a), isometric (b), side (c), and downstream (d) view of the zone 1 injection manifold is shown.

Zone 1 Sampling Manifold

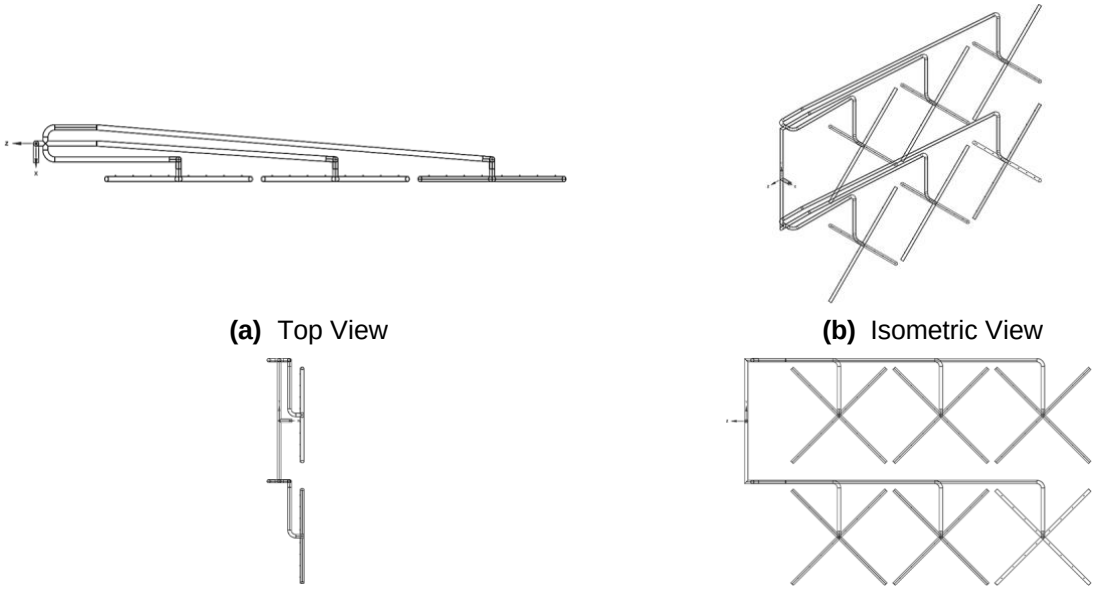

(a) Top View **(b)** Isometric View

(c) Side View **(d)** Downstream View

Figure 1.3: The top (a), isometric (b), side (c), and downstream (d) view of the zone 1 sampling manifold is shown.

Computational Grid

Poly-hexcore meshing was implemented to all grids in this study; the poly-hexcore meshing technique connects high-quality octree hexahedron elements in the bulk region, and isotropic poly-prisms in the boundary layer with mosaic polyhedral elements. This results in an approximately 20% to 50% reduction in the total element count compared to the conventional hexcore meshing technique [1]; poly-hexcore meshing reduces computational costs and solving time.

While generating the grid for each model, sizing functions were used wherever necessary to allow for proper refinement and grid quality. The number of elements is a factor that influences the total computational cost and accuracy of simulation results. Coarse grids create a significant spatial discretization error, thereby reducing the accuracy of the results. In contrast, grids that are too fine may sharply increase the round-off error beyond the truncation error, thereby reducing the accuracy of results. Therefore, it is crucial to create an optimal grid via grid independence study. The grid independence study is a process used to find the optimal grid condition that has the smallest number of elements without generating a significant difference in the numerical results based on the evaluation of various grid conditions. Grid independent solutions do not contain significant discretization or truncation errors. In general, a solution is defined as grid independent if it does not change more than 5% when the number of elements in the grid is approximately doubled [2].

The orthogonal quality was evaluated for each grid. The orthogonal quality evaluates how close the angles between adjacent element faces or edges are to some optimal angle (depending on the topology). The orthogonal quality ranges from 0 (worst) to 1 (best). It is necessary to generate a grid where the element orthogonal qualities are as close to 1 as possible. In general, element

orthogonal quality should not be below 0.10. Elements with an orthogonal quality less than 0.10 could be degenerate – these elements create and propagate large errors and/or convergence issues throughout the simulation [3].

Boundary/inflation layers were added to all walls in each model by evaluating y+ values to properly capture near wall effects. There is a flow region near the walls where the velocity varies logarithmically with distance from the wall; this velocity profile region is the log layer. This behavior is known as the law of the wall [3]. The log layer is where the velocity near the wall is accurately represented. Consequently, to capture the wall effects the mesh near the walls must be adequately refined until the unitless dimension from the wall, y+, falls within the log layer. In general, for viscous dominant flows with separation and no heat transfer, the y+ values should range from 0 to 4 [3].

HEPA Filter Plenum

The grid of the zone 1 HEPA filter plenum is illustrated in Figure 2.1.

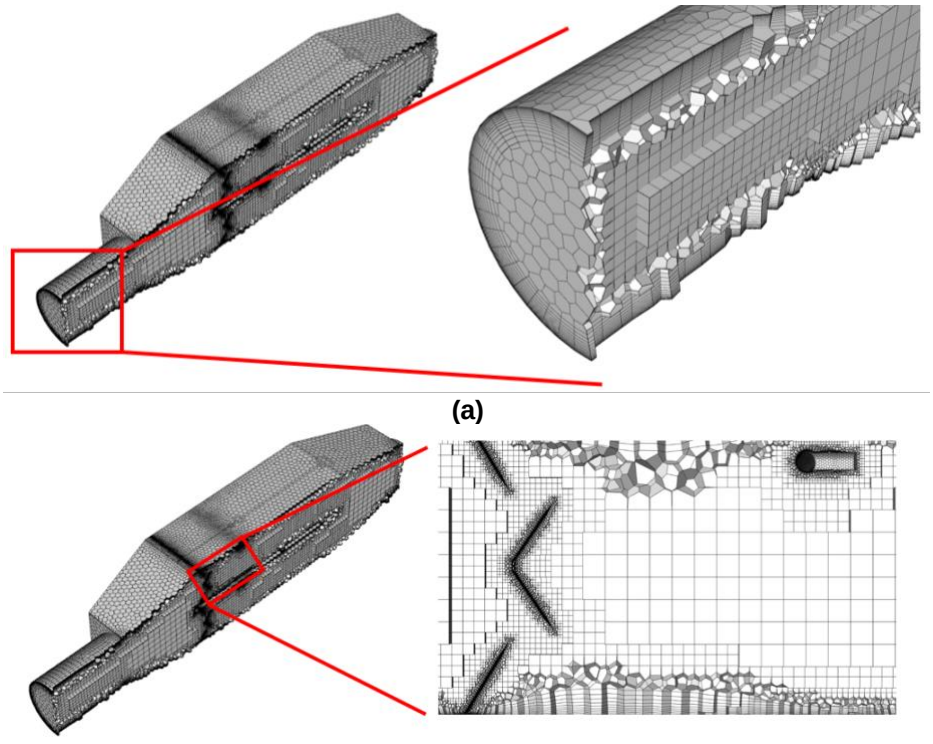

Figure 2.1: The HEPA filter plenum grid is illustrated near the inlet (a), diffusers and pipe (b), and the outlet (c) regions. 15 inflations layers were implemented on all walls.

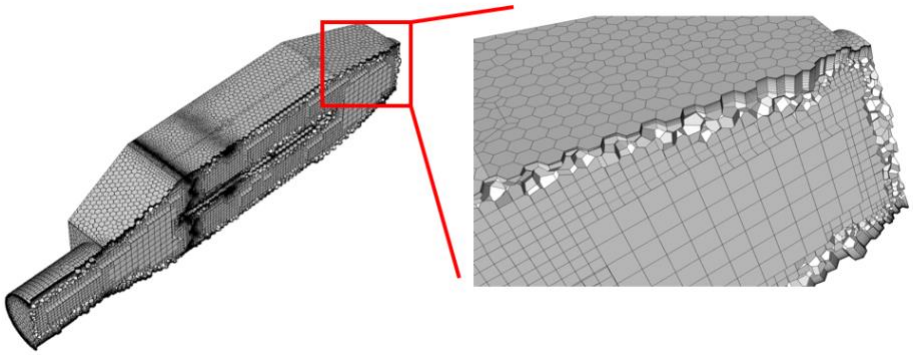

(c)

Figure 2.1: The HEPA filter plenum grid is illustrated near the inlet (a), diffusers and pipe (b), and the outlet (c) regions. 15 inflations layers were implemented on all walls.

The orthogonal quality statistics are summarized in Table 1.1. The average velocity in each bank downstream of the HEPA filter, shown in Figure 2.2, was used to conduct the grid study. All errors are less than 5% and decrease as the number of elements are increased. Therefore, the solution is grid independent. For computational efficiency, the course grid was used for this study. The grid study is summarized in Table 1.2. The min, max, and average y+ values for the HEPA filter plenum are 0.65. 1.58, and 0.93 respectively.

Table 1.1: The summary statistics for the orthogonal quality of each grid generated for the HEPA filter plenum.

Grid	Number of Elements	Min.	Max.	Average
Course	$03.40 \cdot 10^6$	0.19	1.00	0.89
Medium	$07.30 \cdot 10^6$	0.16	1.00	0.86
Fine	$15.61 \cdot 10^6$	0.15	1.00	0.81

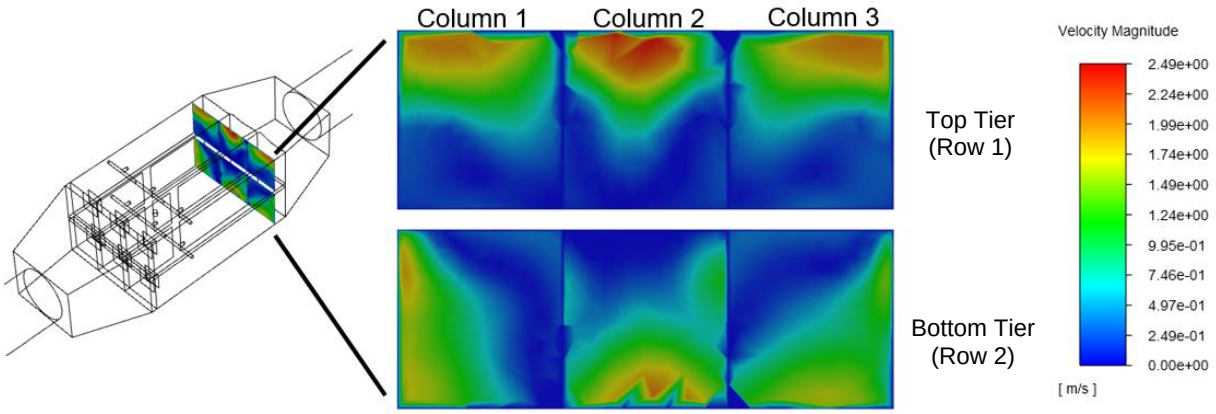

Figure 2.2: The velocity profile resulting from grid 1 in each bank downstream of the HEPA filter.

Table 1.2: Grid study for the HEPA filter plenum.

Plane Section	Grid	Average Velocity [m/s]	Error
Row 1, Column 1	1	0.66	-
	2	0.68	2.94%
	3	0.69	1.45%
Row 1, Column 2	1	0.96	-
	2	0.99	3.03%
	3	1.01	1.52%
Row 1, Column 3	1	0.63	-
	2	0.65	3.08%
	3	0.66	1.52%
Row 2, Column 1	1	0.64	-
	2	0.62	3.23%
	3	0.61	1.64%
Row 2, Column 2	1	0.93	-
	2	0.95	2.11%
	3	0.96	1.04%
Row 2, Column 3	1	0.70	-
	2	0.72	2.78%
	3	0.73	1.37%

Zone 1 Injection Manifold

The grid of the zone 1 injection manifold is illustrated in Figure 3.1.

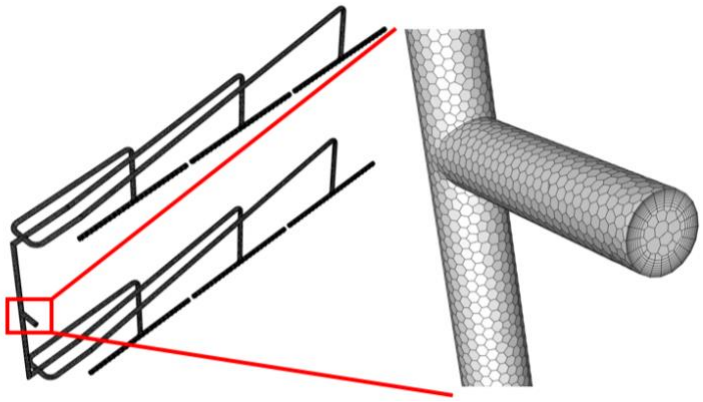

(a)

Figure 3.1: The zone 1 injection manifold grid is illustrated near the inlet (a) and top middle outlet (b) regions. 10 inflations layers were implemented on all walls.

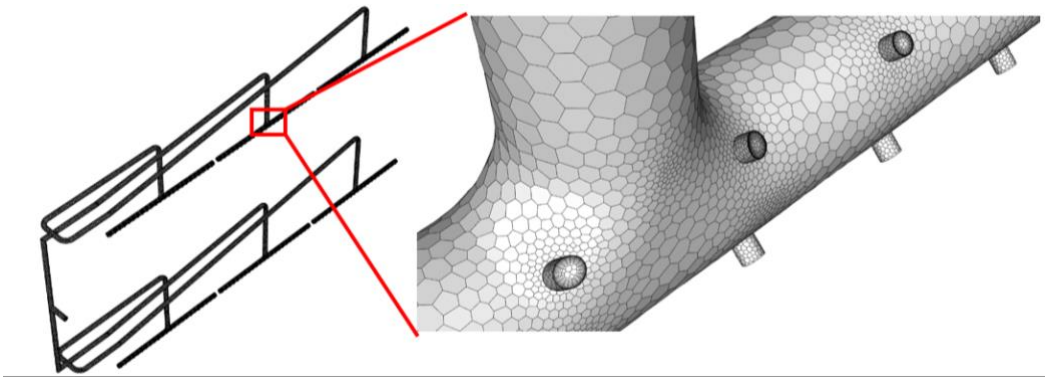

(b)

Figure 3.1: The zone 1 injection manifold grid is illustrated near the inlet (a) and top middle outlet (b) regions. 10 inflations layers were implemented on all walls.

The orthogonal quality statistics are summarized in Table 2.1. The mass flow rate in each injection section, shown in Figure 3.2, was used to conduct the grid study. All errors are less than 5% and decrease as the number of elements are increased. Therefore, the solution is grid independent. For computational efficiency, the course grid was used for this study. The grid study is summarized in Table 2.2. The min, max, and average y+ values for the zone 1 injection manifold are 0.01. 0.70, and 0.14 respectively.

Table 2.1: The summary statistics for the orthogonal quality of each grid generated for the zone 1 injection manifold.

Grid	Number of Elements	Min.	Max.	Average
Course	$02.15 \cdot 10^6$	0.26	1.00	0.92
Medium	$04.53 \cdot 10^6$	0.34	1.00	0.92
Fine	$08.23 \cdot 10^6$	0.25	1.00	0.93

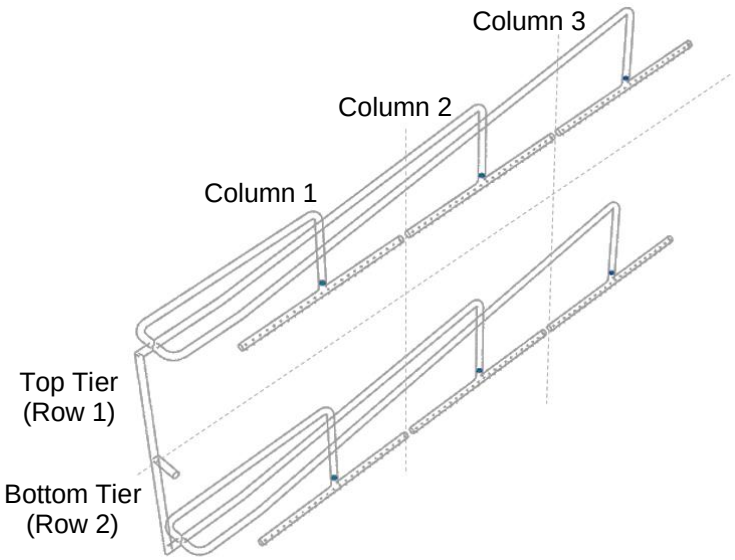

Figure 3.2: The mass flow rate measurement location in each injection section is highlighted in dark blue.

Table 2.2: Grid study for the zone 1 injection manifold.

Injection Section	Grid	Mass Flow Rate [kg/s]	Error
Row 1, Column 1	1	5.856E-06	-
	2	5.998E-06	2.432%
	3	6.093E-06	1.572%
Row 1, Column 2	1	7.734E-06	-
	2	7.934E-06	2.586%
	3	8.083E-06	1.879%
Row 1, Column 3	1	5.694E-06	-
	2	5.917E-06	3.916%
	3	6.032E-06	1.948%
Row 2, Column 1	1	5.654E-06	-
	2	5.863E-06	3.696%
	3	5.991E-06	2.186%
Row 2, Column 2	1	7.732E-06	-
	2	7.906E-06	2.250%
	3	8.017E-06	1.399%
Row 2, Column 3	1	6.072E-06	-
	2	6.312E-06	3.964%
	3	6.498E-06	2.945%

Zone 1 Sampling Manifold

The grid of the zone 1 sampling manifold is illustrated in Figure 4.1.

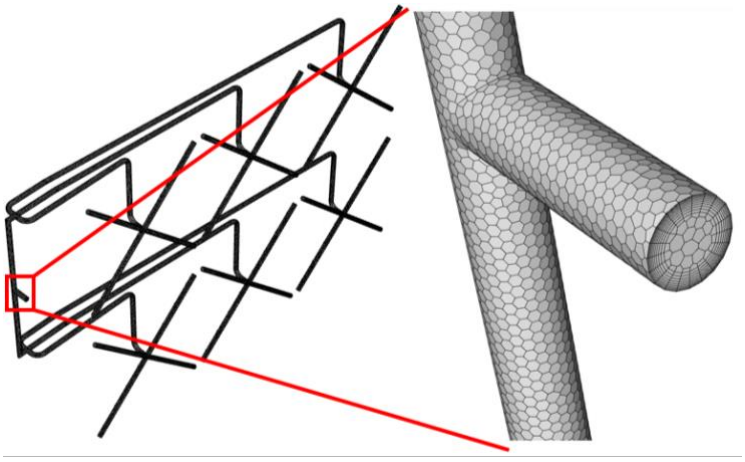

(a)

Figure 4.1: The zone 1 sampling manifold grid is illustrated near the outlet (a) and top middle inlets (b) regions. 10 inflations layers were implemented on all walls.

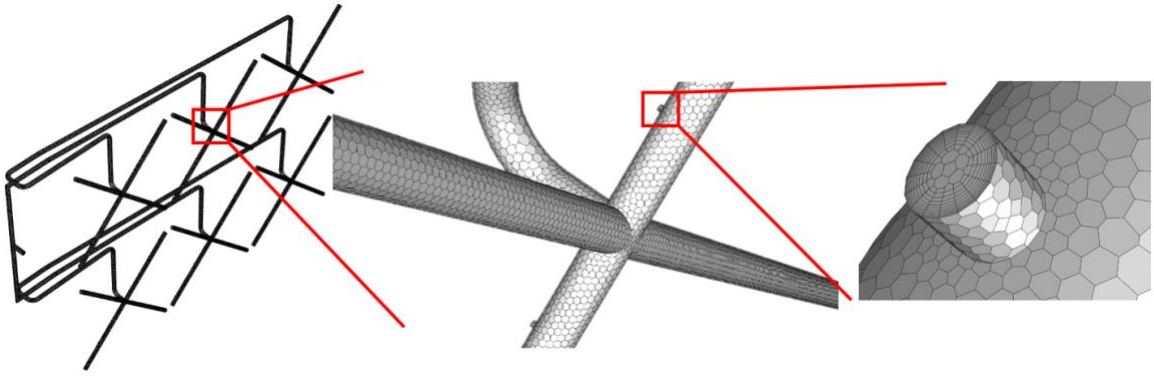

(b)

Figure 4.1: The zone 1 sampling manifold grid is illustrated near the outlet (a) and top middle inlets (b) regions. 10 inflations layers were implemented on all walls.

The orthogonal quality statistics are summarized in Table 3.1. The mass flow rate in each sampling section, shown in Figure 4.2, was used to conduct the grid study. All errors are less than 5% and decrease as the number of elements are increased. Therefore, the solution is grid independent. For computational efficiency, the course grid (grid 1) was used for this study. The grid study is summarized in Table 3.2. The min, max, and average y+ values for the zone 1 sampling manifold are 0.01. 0.74, and 0.15 respectively.

Table 3.1: The summary statistics for the orthogonal quality of each grid generated for the zone 1 sampling manifold.

Grid	Number of Elements	Min.	Max.	Average
Course	$02.25 \cdot 10^6$	0.40	1.00	0.95
Medium	$04.75 \cdot 10^6$	0.43	1.00	0.94
Fine	$09.96 \cdot 10^6$	0.44	1.00	0.95

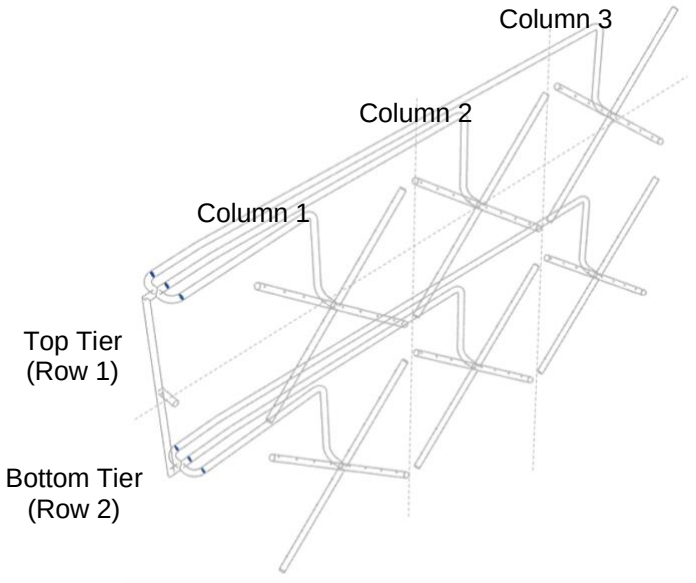

Figure 4.2: The mass flow rate measurement location in each sampling section is highlighted in dark blue.

Table 3.2: Grid study for the zone 1 sampling manifold.

Sampling Section	Grid	Mass Flow Rate [kg/s]	Error
Row 1, Column 1	1	6.41E-05	-
	2	6.64E-05	3.483%
	3	6.73E-05	1.338%
Row 1, Column 2	1	5.47E-05	-
	2	5.66E-05	3.601%
	3	5.75E-05	1.573%
Row 1, Column 3	1	4.65E-05	-
	2	4.89E-05	5.104%
	3	4.95E-05	1.233%
Row 2, Column 1	1	6.35E-05	-
	2	6.56E-05	3.188%
	3	6.67E-05	1.673%
Row 2, Column 2	1	5.44E-05	-
	2	5.69E-05	4.638%
	3	5.79E-05	1.639%
Row 2, Column 3	1	4.63E-05	-
	2	4.87E-05	5.073%
	3	4.99E-05	2.468%

Boundary Conditions

The boundary conditions for each model in this study is provided in this section.

HEPA Filter Plenum

The definitions of the HEPA filter plenum's fluid boundaries are illustrated in Figure 5. Air (with density and dynamic viscosity of 0.931 kg/m^3 and 1.789E-5 kg/m-s, respectively) was used as the simulated fluid. The boundary conditions for the HEPA filter plenum are summarized in Table 4.

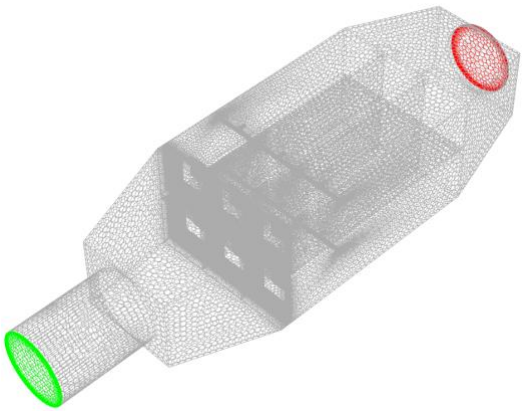

Figure 5: The boundary conditions for the HEPA filter plenum are defined. The inlet and outlet are shown in green and red, respectively. All other surfaces are defined as non-slip walls.

Table 4: The boundary conditions of the HEPA filter plenum simulation.

Parameter	Velocity Inlet	Pressure Outlet	Walls
Velocity	3.0207 m/s	-	Stationary, No Slip
Pressure	77007 Pa (Initial Gauge)	75424 Pa (Absolute Gauge)	-
Turbulence Intensity	5.000%	5.000%	-
Hydraulic Diameter	0.9144 m	0.9144 m	-

Zone 1 Injection Manifold

The definitions of the zone 1 injection manifold's fluid boundaries are illustrated in Figure 6. Polyalphaolefin 4 (PAO-4 with density and dynamic viscosity of 0.622 kg/m^3 and 9.952E-06 kg/m-s, respectively) were used as the simulated fluids. The boundary conditions for the zone 1 injection manifold are summarized in Table 5.

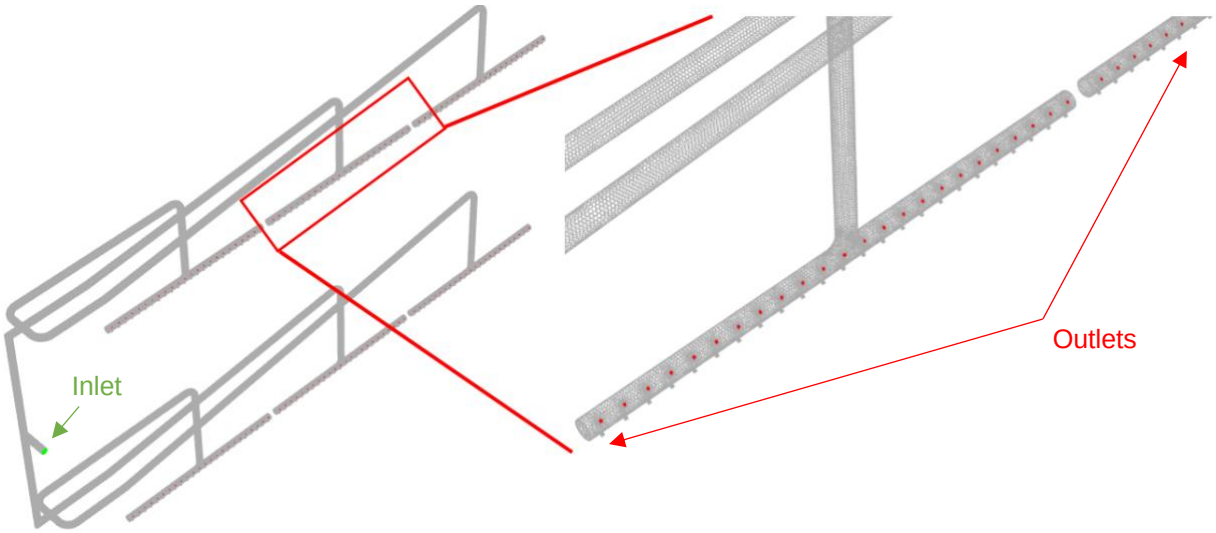

Figure 6: The boundary conditions for the zone 1 injection manifold are defined. The inlet and outlet are shown in green and red, respectively. There is a total of 288 outlet faces across all six injection sections. All other surfaces are defined as non-slip walls.

Table 5: The boundary conditions of the zone 1 injection manifold simulation.

Parameter	Velocity Inlet	Pressure Outlet	Walls
Velocity	0.17099 m/s	-	Stationary, No Slip
Pressure	77007 Pa (Initial Gauge)	75424 Pa (Absolute Gauge)	-
Turbulence Intensity	5.000%	5.000%	-
Turbulent Viscosity Ratio	10	10	-

Zone 1 Sampling Manifold

The definitions of the zone 1 sampling manifold's fluid boundaries are illustrated in Figure 7. The simulated fluid has a density and dynamic viscosity of 0.735 kg/m^3 and 1.789E-05 kg/m-s, respectively. The fluid density was estimated as the average density of the mixture between PAO-4 and air upstream of the sampling manifold location. The dynamic viscosity of air is used for the

fluid as the majority of the fluid mixture is air. The boundary conditions for the zone 1 sampling manifold are summarized in Table 6.

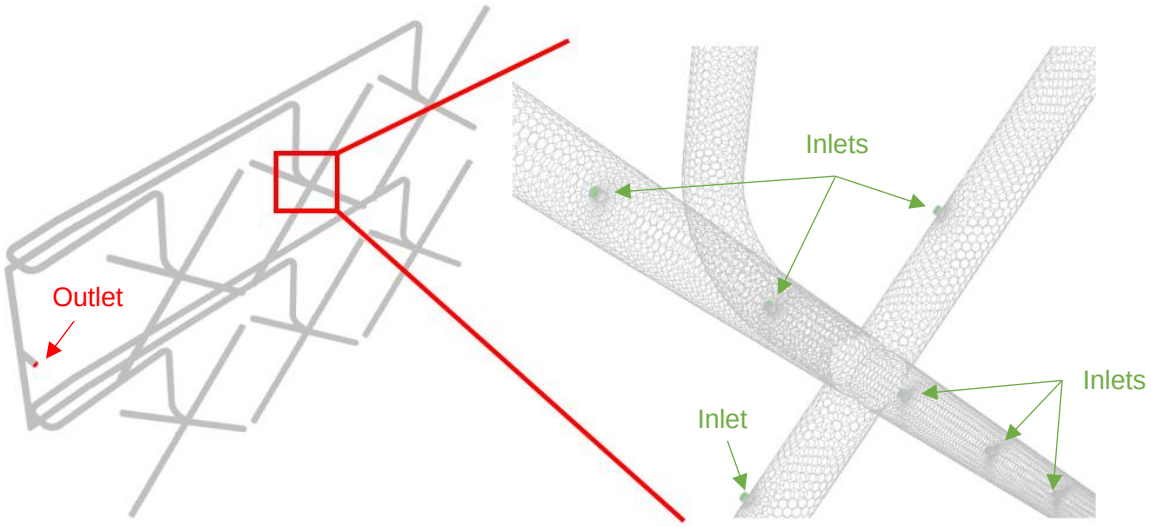

Figure 7: The boundary conditions for the zone 1 sampling manifold are defined. The inlet and outlet are shown in green and red, respectively. There is a total of 98 inlet faces across all six sampling sections. All other surfaces are defined as non-slip walls.

Table 6: The boundary conditions of the zone 1 sampling manifold simulation.

Parameter	Pressure Inlet	Velocity Outlet	Walls
Velocity	-	1.3679 m/s	Stationary, No Slip
Pressure	75424 Pa (Absolute Gauge)	77007 Pa (Initial Gauge)	-
Turbulence Intensity	5.000%	5.000%	-
Turbulent Viscosity Ratio	10	10	-

Solver Settings

For all models in this study, a coupled pressure-based solver was used where the pressure, momentum, turbulent kinetic energy, and turbulent dissipation rate were solved by second order schemes. The pseudo transient scheme was also enforced. To help accelerate the solution, a hybrid initialization was used and the number of iterations was limited to 500.

The shear stress transport (SST) k-omega viscous model was used for all simulations in this study. The SST k-omega turbulence model is a variant of the standard k-omega model while also incorporating the formulation of the standard k-epsilon model. The standard k-omega model demonstrates superior performance for wall bounded and low Reynolds number flows. It has high potential for predicting flow transition and also accounts for free shear and compressible flows. The standard k-epsilon model is valid for fully turbulent flows only and performs poorly for complex flows involving severe pressure gradients, separation, and strong streamline curvature. The SST k-omega model employs the standard k-omega formulation in the inner parts of the boundary layer which makes the model directly usable towards the wall through the viscous sub-layer. Consequently, the SST k-omega model can be used as a low Reynolds turbulence model without any extra damping functions. The SST formulation also switches to a standard k-epsilon behavior

in the free-stream and thereby avoids a common standard k-omega problem – high sensitivity to inlet free-stream turbulence properties [3].

The convergence criteria for all simulations in this study were for all residuals to be less than or equal to 1E-3. The plots of all residuals for each model in this study are provided in Figures 8.1, 8.2, and 8.3.

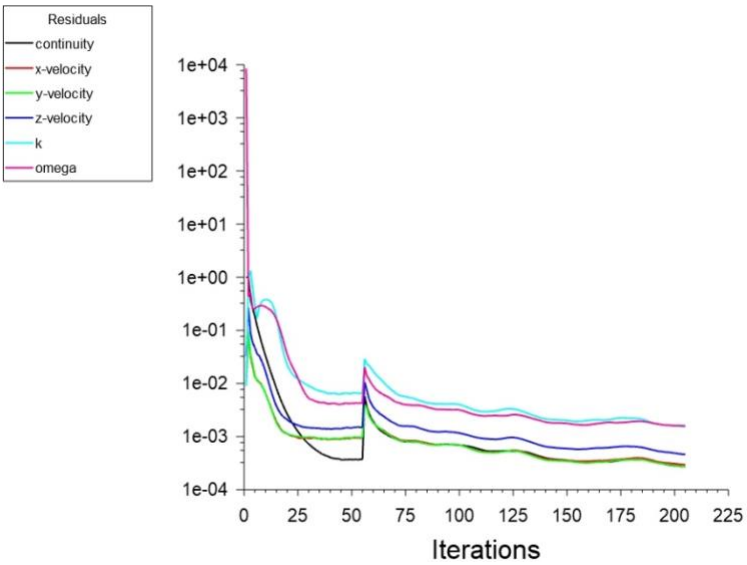

Figure 8.1: The converged residuals for the HEPA filter plenum. First order schemes were initially implemented then convergence was achieved by initializing second order schemes using the first order solutions.

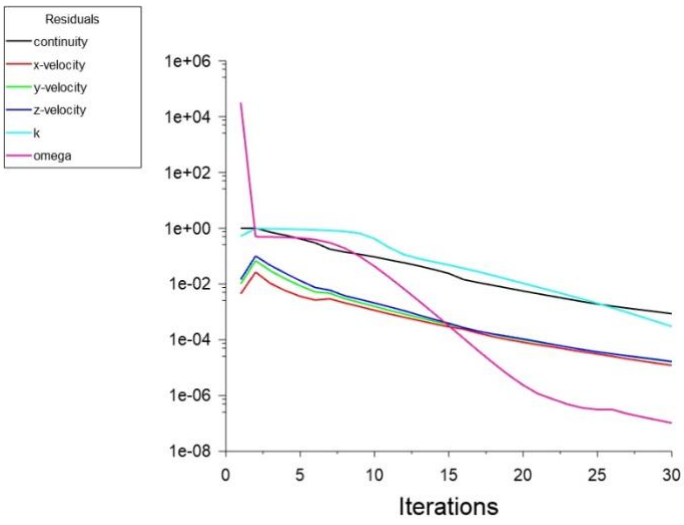

Figure 8.2: The converged residuals for the zone 1 injection manifold.

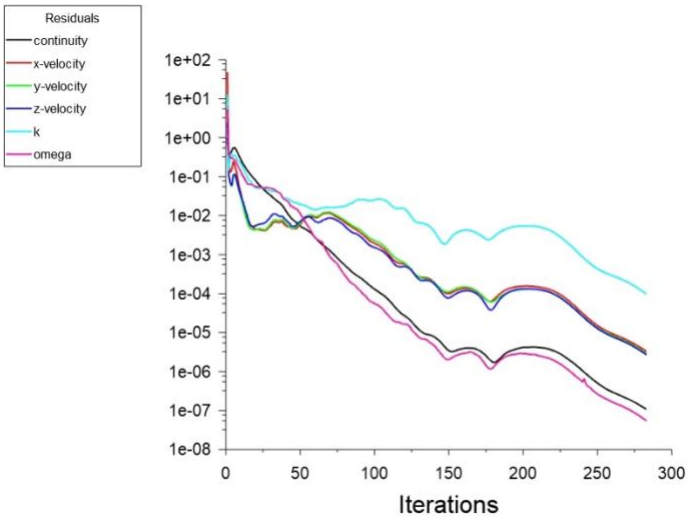

Figure 8.3: The converged residuals for the zone 1 sampling manifold.

Results

HEPA Filter Plenum

Global velocity contour planes of the HEPA filter plenum are illustrated in Figure 9.1 and 9.2. The min, max, and average velocities on the plane in each bank downstream from the HEPA filter are reported in Table 7.1 and the percent change from the average of the min and max velocities of the respective plane are provided in Table 7.2. The average velocities and mass flow rates of a plane upstream of the HEPA filter are summarized in Table 7.3.

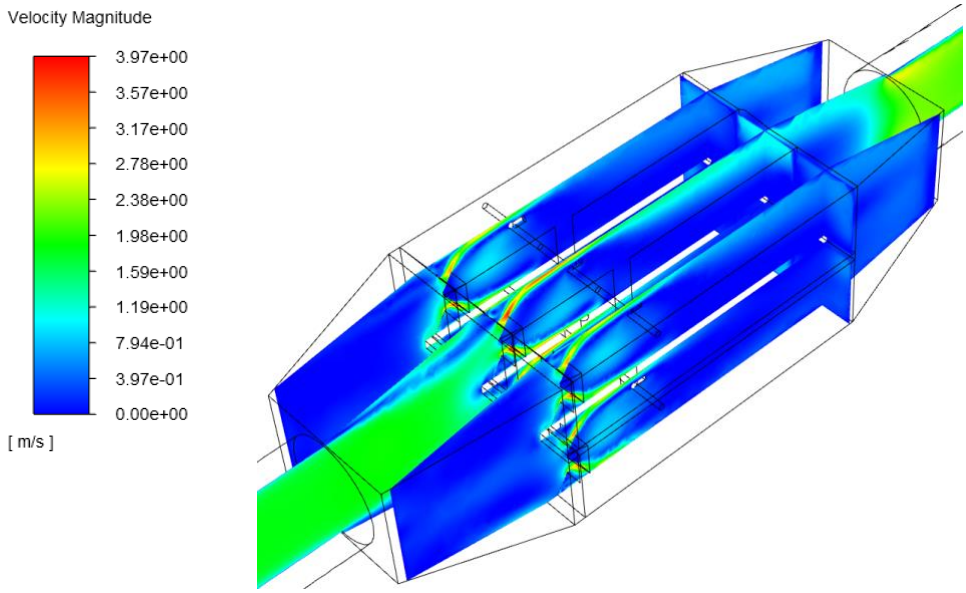

Figure 9.1: Global contour planes of the HEPA filter plenum are shown.

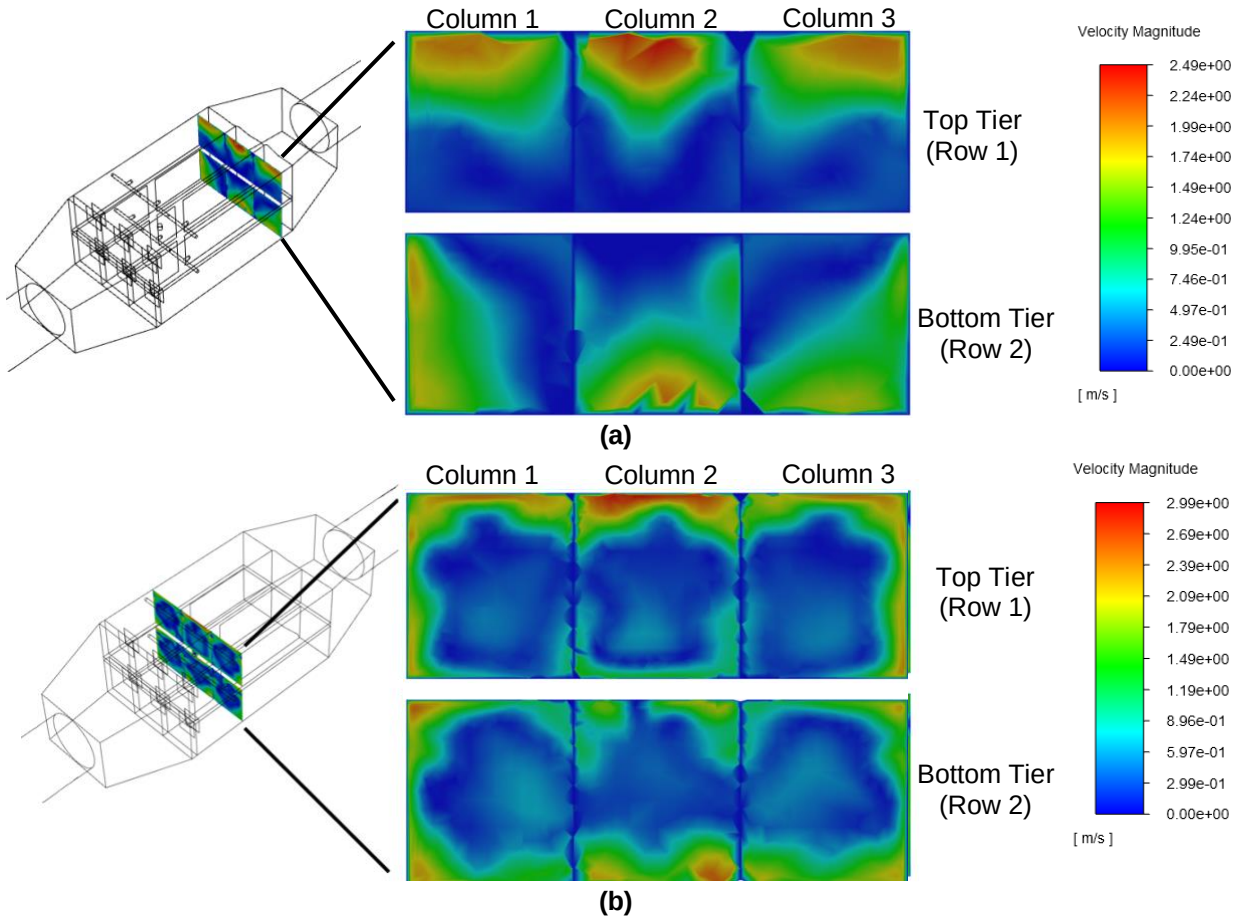

Figure 9.2: The velocity profile in each bank downstream (a) and upstream (b) of the HEPA filter is shown.

Table 7.1: The min, max, and average velocities in m/s on the plane in each bank downstream from the HEPA filter.

Plane Section	Min.	Max.	Average
Row 1, Column 1	0.00	1.74	0.66
Row 1, Column 2	0.00	2.87	0.96
Row 1, Column 3	0.00	1.33	0.63
Row 2, Column 1	0.00	1.68	0.64
Row 2, Column 2	0.00	2.68	0.93
Row 2, Column 3	0.00	1.47	0.70

Table 7.2: The percent change from the average of the min and max velocities on the plane in each bank downstream from the HEPA filter.

Plane Section	Min: Deviation from Average	Max: Deviation from Average
Row 1, Column 1	-100%	163%
Row 1, Column 2	-100%	199%
Row 1, Column 3	-100%	111%
Row 2, Column 1	-100%	163%
Row 2, Column 2	-100%	188%
Row 2, Column 3	-100%	110%

Table 7.3: The average velocities and mass flow rates of a plane upstream of the HEPA filter.

Plane Section	Average Velocity [m/s]	Mass Flow Rate [kg/s]
Row 1, Column 1	0.69	0.313
Row 1, Column 2	0.97	0.324
Row 1, Column 3	0.68	0.305
Row 2, Column 1	0.67	0.368
Row 2, Column 2	0.95	0.394
Row 2, Column 3	0.73	0.345

Zone 1 Injection Manifold

The average mass flow rate across all injection sections is 6.450E-06 kg/s. The mass flow rates in each section of the injection manifold and its deviation from the average are summarized in Table 8.1. The mass flow rate measurement location in each injection section is shown in Figure 3.2.

Table 8.1: The mass flow rates in each section of the injection manifold. The average mass flow rate across all injection sections is 6.450E-06 kg/s.

Injection Section	Mass Flow Rate [kg/s]	Deviation from Average
Row 1, Column 1	5.853E-06	09.31%
Row 1, Column 2	7.722E-06	19.78%
Row 1, Column 3	5.679E-06	11.81%
Row 2, Column 1	5.654E-06	12.43%
Row 2, Column 2	7.728E-06	19.74%
Row 2, Column 3	6.065E-06	05.97%

Zone 1 Sampling Manifold

The average mass flow rate across all sampling sections is 5.492E-05 kg/s. The mass flow rates in each section of the sampling manifold and its deviation from the average are summarized in Table 8.2. The mass flow rate measurement location in each sampling section is shown in Figure 4.2.

Table 8.2: The mass flow rates in each section of the sampling manifold. The average mass flow rate across all injection sections is 5.492E-05 kg/s.

Sampling Section	Mass Flow Rate [kg/s]	Deviation from Average
Row 1, Column 1	6.41E-05	14.35%
Row 1, Column 2	5.47E-05	00.49%
Row 1, Column 3	4.65E-05	18.01%
Row 2, Column 1	6.35E-05	13.55%
Row 2, Column 2	5.44E-05	00.98%
Row 2, Column 3	4.63E-05	18.63%

Air-Aerosol Concentration

In realistic working conditions, the zone 1 injection manifold is located inside of the zone 1 HEPA filter plenum, upstream of the HEPA filter. The average velocities and mass flow rates reported in Table 7.3 are upstream of the zone 1 injection manifold and the HEPA filter locations. The injection manifold mass flow rates are summarized in Table 8.1. Figure 10.1 illustrates the relative injection manifold and HEPA filter locations.

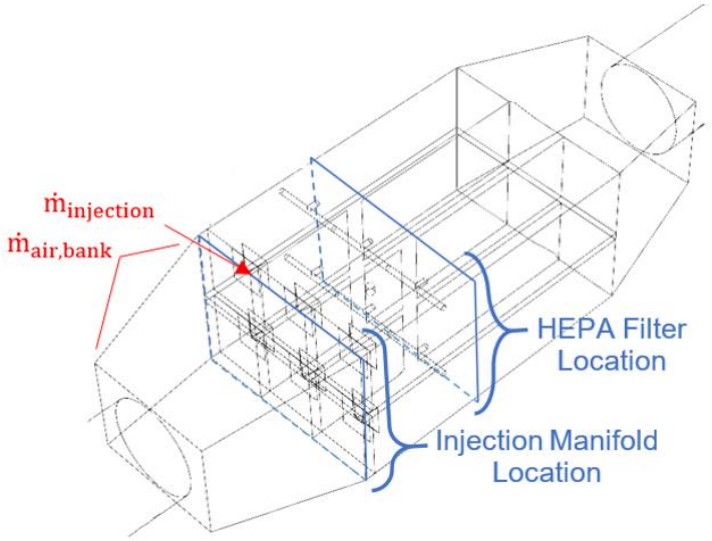

Figure 10.1: The relative locations of the HEPA filter and injection manifold within the zone 1 plenum and the effective mass flow rate locations are illustrated.

The aerosol concentration in each plenum bank section, $A_{con_{i,j}}$, was calculated using Equation 1:

$$A_{con_{i,j}} = \frac{\dot{m}_{injection_{i,j}}}{\bar{v}_{i,j} \cdot A} \qquad \text{Eq. 1}$$

where $\dot{m}_{injection_{i,j}}$ is the mass flow rate of the injection manifold, $\bar{v}_{i,j}$ is the average velocity of a plane upstream of the injection manifold (see Table 7.3) and "$A = 0.435\ m^2$" is the cross-sectional area of each plenum bank; here, *i* is the row and *j* is the column of the measurement location. The aerosol concentration in each plenum bank is summarized in Table 8.3. The average aerosol concentration across all banks is 19.1 μg/L. The aerosol concentration deviation from the average of the respective row is provided in Table 8.4.

Table 8.3: The aerosol concentration in each plenum bank is summarized. The average aerosol concentration across all banks is 19.1 μg/L.

Plenum Bank Section	Aerosol Concentration ($A_{con_{i,j}}$) [μg/L]	Average Concentration [μg/L]
Row 1, Column 1	19.5	19.1
Row 1, Column 2	18.3	
Row 1, Column 3	19.3	
Row 2, Column 1	19.4	
Row 2, Column 2	18.7	
Row 2, Column 3	19.1	

Table 8.4: The aerosol concentration deviation from the average of the respective row.

Plenum Bank Section	Deviation from Average
Row 1, Column 1	1.53%
Row 1, Column 2	2.42%
Row 1, Column 3	0.66%
Row 2, Column 1	1.16%
Row 2, Column 2	1.15%
Row 2, Column 3	0.22%

Conclusions and Discussion

A numerical simulation of airflow in the zone 1 HEPA filter plenum and RLUOB testing manifolds using the commercial CFD software ANSYS FLUENT® 2020R1 was presented. The CFD analysis focused on the investigation of the air flow distribution and air-aerosol mixing uniformity. The evaluation was done for all steps of the modeling process: grid generation, physics setup, simulation, and post-processing. The mass flow rate in each section of the zone 1 injection and sampling manifolds is also reported.

ASME AG-1 has two requirements:

1. The variation in velocity measurements across the HEPA filter banks (downstream) shall be limited to limited to ±20% of the average velocity in each bank.

2. The variation in concentration of the air-aerosol mixture immediately upstream of the HEPA filter bank shall be limited to $\pm$20% of the average concentration across all adjacent banks.

The velocity contours for the HEPA filter plenum are provided in Figures 9.1 and 9.2. Table 7.2 shows that the variation in velocity measurements across the HEPA filter banks (downstream)

are greater than ±20% of the average velocity in each bank. Consequently, the CFD analysis shows that requirement 1 is not satisfied. However, the respective CFD analysis does not capture the HEPA filter physics. In reality, HEPA filters equalize the flow and greatly dissipate the velocity due to their large, condensed, surface area. Therefore, the verification of ASME AG-1 requirement 1 is inclusive by this CFD study.

The aerosol concentration upstream of the HEPA filter location was calculated using the velocity profiles and mass flow rates of the HEPA filter plenum and zone 1 injection manifold. The plenum velocity profiles upstream of the HEPA filter is illustrated in Figure 9.2 and summarized in Table 7.3. The injection manifold mass flow rates are summarized in Table 8.1.

Table 8.4 shows that the variation in concentration of the air-aerosol mixture immediately upstream of the HEPA filter bank is less than 3% of the average concentration across all adjacent filters on that tier. The lack of HEPA filter physics does not significantly affect the concentration results because the flow is upstream of the HEPA filter. Consequently, ASME AG-1 requirement 2 is satisfied.

References

[1] K. Zore, G. Parkhi, B. Sasanapuri and A. Varghese, "ANSYS Mosaic Poly-Hexcore Mesh for High-Lift Aircraft Configuration," in *21stAnnual CFD Symposium*, Bangalore, 2019.

[2] M. Lee, G. Park, C. Park and C. Kim, "Improvement of GridIndependence Test for Computational Fluid Dynamics Model of Building Based on Grid Resolution," *Hindawi,* vol. 2020, 2020.

[3] J. Ferziger and M. Peric, Computational Methods for Fluid Dynamics, New York: Springer, 2002.

Attachment(s): Attachment 1: Geometry Dimensions
Attachment 2: Zone 1 – 3 Effective Injection Manifolds Analysis
Attachment 3: Zone 1 – 3 Effective Sampling Manifolds Analysis

Copy: Andrea, Gerber, ES-EPD, agerber@lanl.gov
Thad, Hahn, ES-CWF, twhahn@lanl.gov
Martin, Davis, ES-CWF, mdavis@lanl.gov
Todd, Smith, ES-EDP, toddsmith@lanl.gov
Bob, Griffis, ES-CWF, rgriffis@lanl.gov
Scott, Salisburry, ES-55, salisbury_scott_r@lanl.gov
Mike, Flores, ETD-E1, flores@lanl.gov

Attachment 1: Geometry Dimensions

The dimensions of the internal volume (fluid domain) of all geometries used in this study is provided here. All dimensions are in inches.

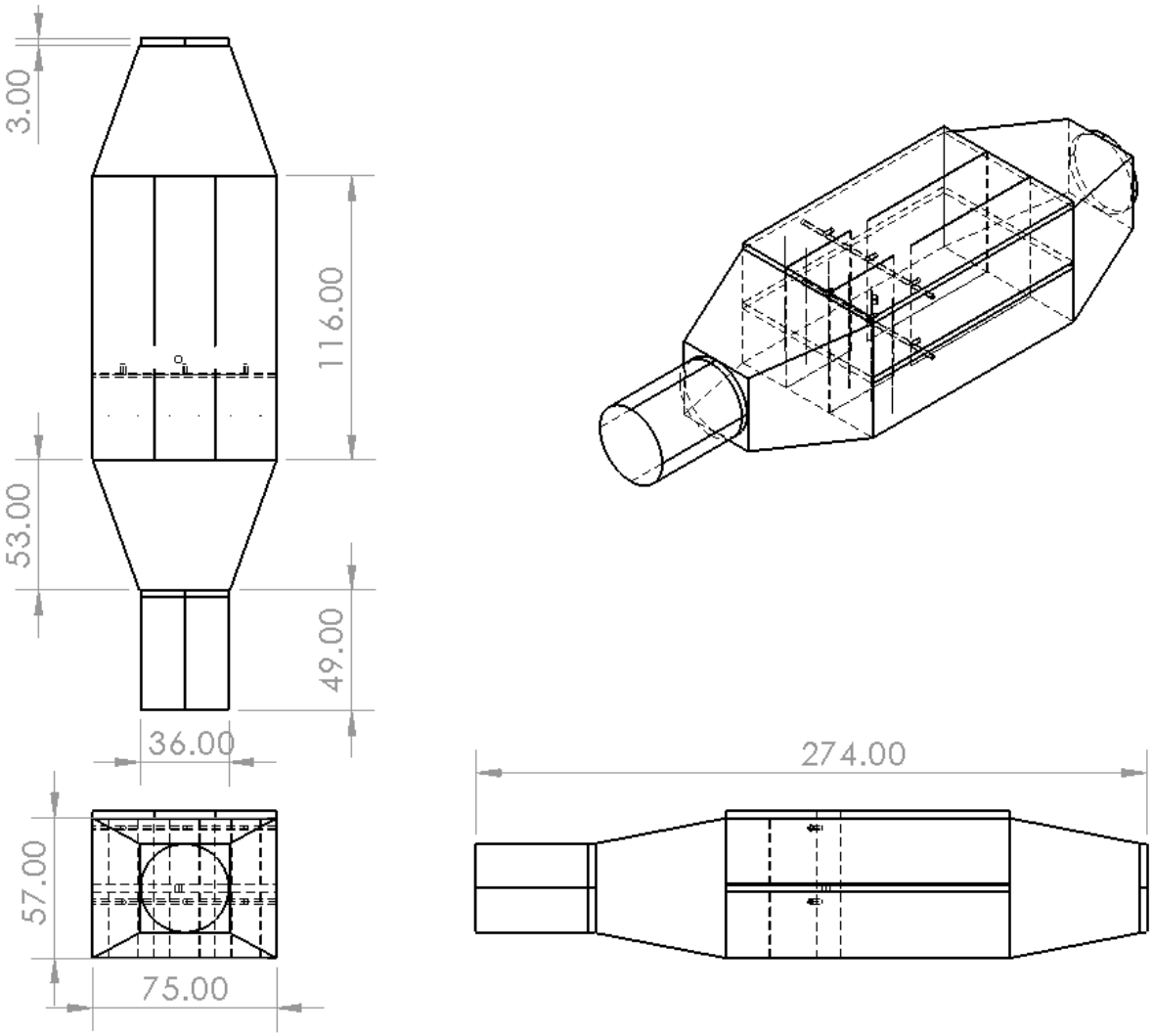

Figure A.1.1: General dimensions of the internal volume of the HEPA filter plenum.

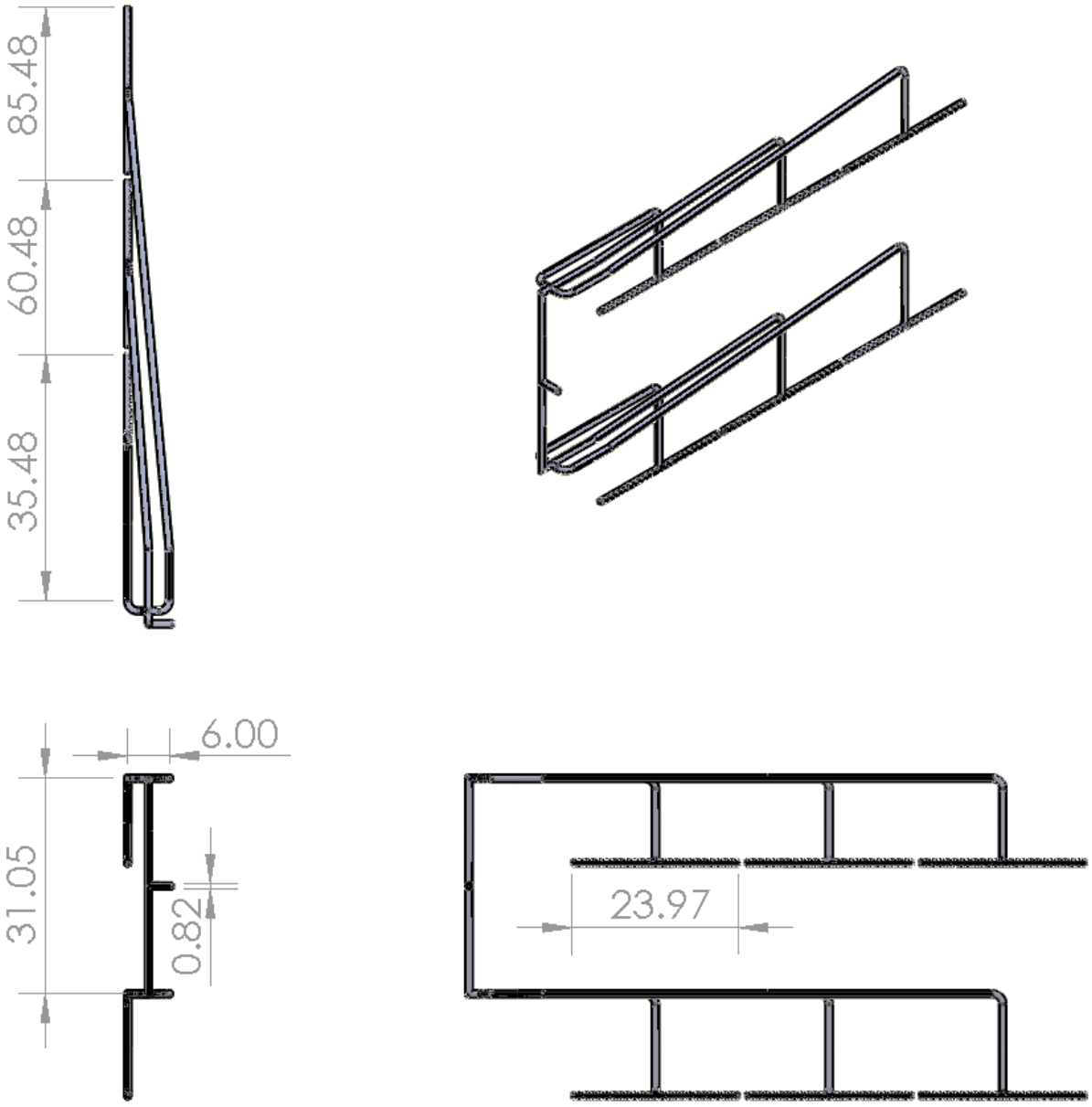

Figure A.1.2: General dimensions of the internal volume of the zon1 injection manifold.

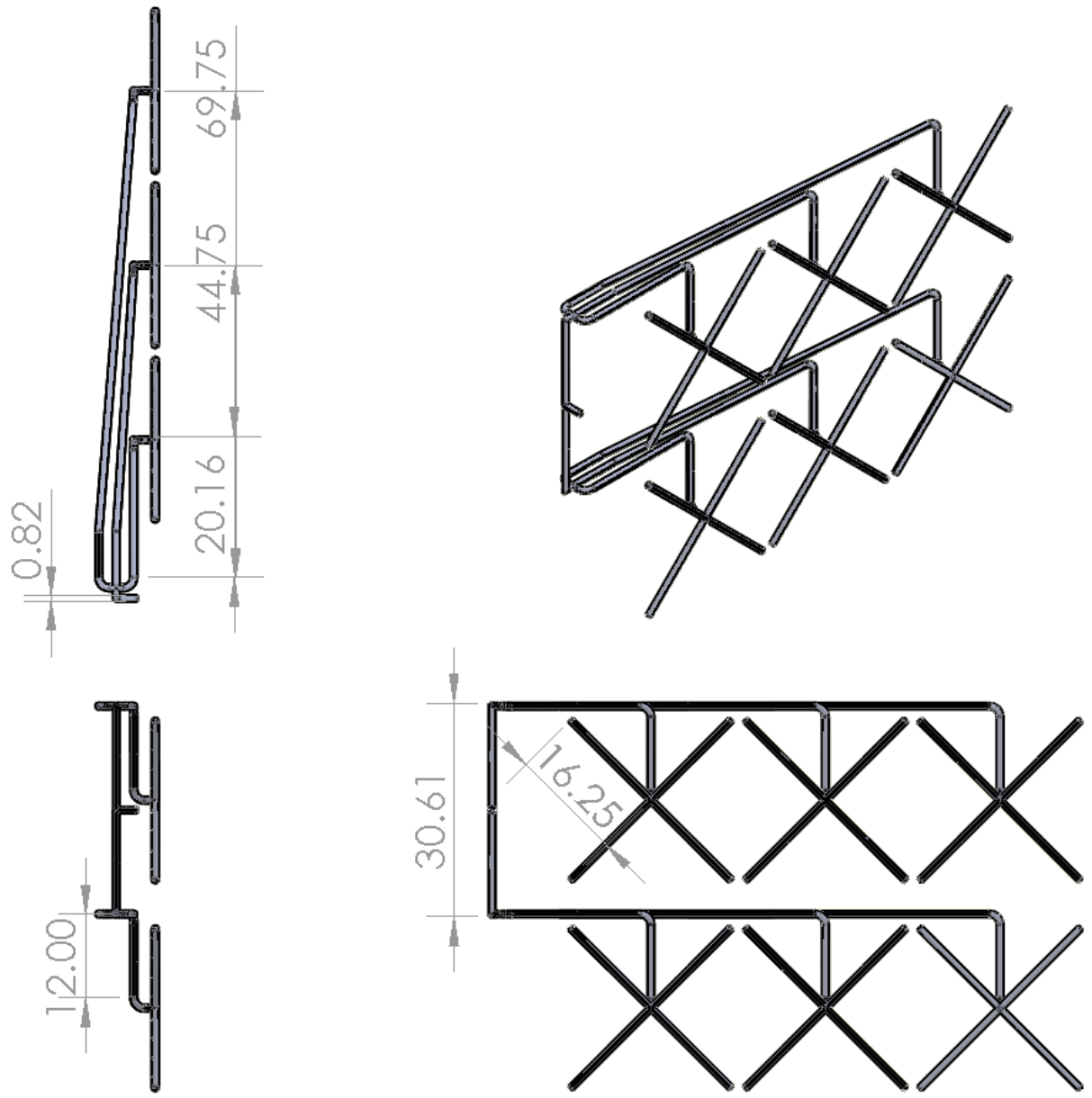

Figure A.1.3: General dimensions of the internal volume of the zone 1 sampling manifold.

Attachment 2: Zone 1 – 3 Effective Injection Manifolds Analysis

Grid Study

The medium grid was used in this study.

Table A.2.1: The summary statistics for the orthogonal quality of each grid generated for the zone 1 injection manifold.

Grid	Number of Elements	Min.	Max.	Average
Course	$1.31 \cdot 10^6$	0.32	1.00	0.92
Medium	$2.75 \cdot 10^6$	0.42	1.00	0.93
Fine	$5.56 \cdot 10^6$	0.44	1.00	0.93

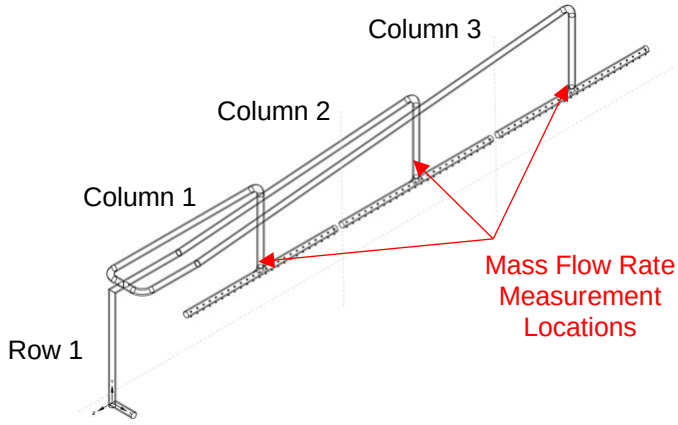

Figure A.2.1: The mass flow rate measurement location in each injection section is shown.

Table A.2.2: Grid study for the zone 1 injection manifold.

Injection Section	Grid	Mass Flow Rate [kg/s]	Error
Row 1, Column 1	1	1.19E-05	-
	2	1.22E-05	2.271%
	3	1.23E-05	1.069%
Row 1, Column 2	1	1.56E-05	-
	2	1.60E-05	2.497%
	3	1.63E-05	1.562%
Row 1, Column 3	1	1.15E-05	-
	2	1.19E-05	3.649%
	3	1.21E-05	1.509%

Results

Table A.2.3: The mass flow rates in each section of the injection manifold.

Sampling Section	Mass Flow Rate [kg/s]
Row 1, Column 1	1.085E-04
Row 1, Column 2	1.084E-04
Row 1, Column 3	6.864E-05

Attachment 3: Zone 1 – 3 Effective Sampling Manifolds Analysis

Grid Study

The medium grid was used in this study.

Table A.3.1: The summary statistics for the orthogonal quality of each grid generated for the zone 1 sampling manifold.

Grid	Number of Elements	Min.	Max.	Average
Course	$1.11 \cdot 10^6$	0.47	1.00	0.94
Medium	$2.23 \cdot 10^6$	0.45	1.00	0.93
Fine	$4.78 \cdot 10^6$	0.43	1.00	0.93

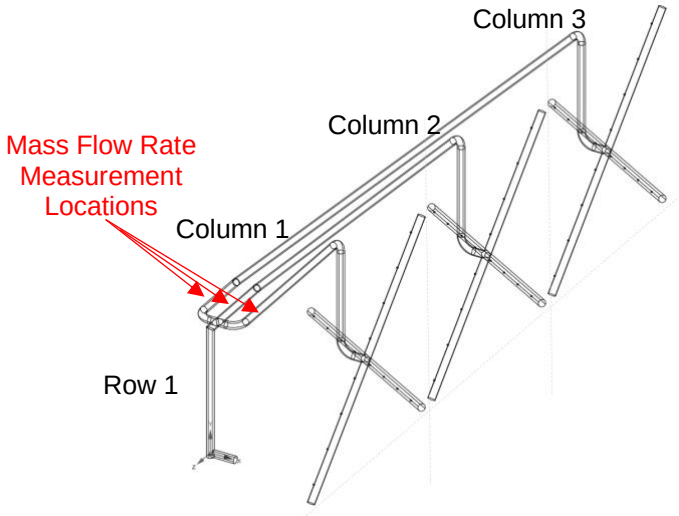

Figure A.3.1: The mass flow rate measurement location in each sampling section is shown.

Table A.3.2: Grid study for the zone 1 sampling manifold.

Sampling Section	Grid	Mass Flow Rate [kg/s]	Error
Row 1, Column 1	1	3.318E-05	-
	2	3.452E-05	4.035%
	3	3.559E-05	3.079%
Row 1, Column 2	1	2.832E-05	-
	2	2.958E-05	4.464%
	3	2.996E-05	1.285%
Row 1, Column 3	1	2.446E-05	-
	2	2.542E-05	3.930%
	3	2.601E-05	2.317%

Results

Table A.3.3: The mass flow rates in each section of the sampling manifold.

Sampling Section	Mass Flow Rate [kg/s]
Row 1, Column 1	3.318E-05
Row 1, Column 2	2.832E-05
Row 1, Column 3	2.446E-05